RSC Advances

PAPER

View Article Online
View Journal | View Issue

Cite this: *RSC Adv.*, 2020, **10**, 17079

An ionic diode based on a spontaneously formed polypyrrole-modified graphene oxide membrane†

Rifeng Luo,‡[a] Tianliang Xiao,‡[a] Wenping Li,*[b] Zhaoyue Liu *[a] and Yao Wang *[c]

Received 6th February 2020
Accepted 24th April 2020

DOI: 10.1039/d0ra01145b

rsc.li/rsc-advances

Asymmetric membranes derived from the stacking of graphene oxide (GO) nanosheets have attracted great attention for the fabrication of ionic diodes. Herein, we described an ionic diode based on a polypyrrole-modified GO membrane with a vertical asymmetry, which was achieved by a spontaneous oxidation polymerization of pyrrole monomers on one side of the GO membrane in vapor phase. This asymmetric modification resulted in an asymmetric geometry due to the occupation of the interlayer space of one side of the GO membrane by polypyrrole. Our ionic diode demonstrated an obvious ionic rectification behavior over a wide voltage range. A calculation based on Poisson–Nernst–Planck equations was used to theoretically investigate the role of asymmetric modification of polypyrrole.

1. Introduction

Ionic diodes that rectify the ionic current through nanometer-scale channels in one direction (*i.e.* a nonlinear current–voltage curve) receive considerable interest because of their potential applications such as in biosensors, molecular separation and energy conversion.[1–20] The discovery of ionic diodes is considered to be inspired by biological ion channels with an asymmetric charge distribution along the fluidic channels.[21,22] When the radius of fluidic channels in ionic diodes is comparable to the Debye length of the electrolyte, the asymmetric distribution of electric field along the fluidic channels allows the flow of ions in one direction preferentially.[23] Such a charge asymmetry has been achieved by fixing homogeneous surface charges in geometry-asymmetric fluidic channels[24–29] or introducing non-homogeneous charge patterns in geometry-symmetric fluidic channels,[30–36] or the combination of both.[37–40]

Layered membranes derived from the stacking of graphene oxide (GO) nanosheets by a vacuum filtration have attracted great attention for the fabrication of ionic diodes.[41–47] The negatively charged surface of GO nanosheets by carboxylic groups enable the interlayer spaces between nanosheets function as fluidic channels to control the ionic transport.[48,49] Recently, the asymmetric GO layered membrane has been used to fabricate ionic diodes. Several examples of planar ionic diodes based on tailor-cutted GO membrane with a lateral asymmetry have been reported.[41–43] It has been noticed that the asymmetrization of GO membrane in a vertical dimension is another key issue because the surface of GO membrane can provide a large and tunable flux for ion transport when compared with its cross section. For example, the deposition of spiropyran moieties on one side of GO membrane enabled it to rectify ion transport effectively.[44] The sequential stacking of negatively and positively charged GO membrane also rectified the ion transport.[45,46] Therefore, the development of an alternative GO membrane with a vertical asymmetry is of significant importance for the fabrication of ionic diodes.

Conducting polymer such as polypyrrole is one kind of effective materials for the development of ionic diode as reported by our and other groups' work.[50–54] Herein, we described an ionic diode based on a polypyrrole-modified GO membrane with a vertical asymmetry, which was achieved by a spontaneous oxidation polymerization of pyrrole monomer on one side of GO membrane in vapor phase at ambient temperature. The asymmetric modification resulted in an asymmetric geometry due to the occupation of interlayer space of one side of GO membrane by polypyrrole. Our ionic diode demonstrated an obvious ionic rectification behavior over a wide voltage range, which was subsequently explained by a theoretical calculation based on Poisson–Nernst–Planck equations.

2. Results and discussion

GO nanosheets exfoliated from graphite by a modified Hummers' method are intrinsically decorated by carboxyl, hydroxyl and epoxy groups, which can be stacked into high-

[a]*Key Laboratory of Bio-Inspired Smart Interfacial Science and Technology of Ministry of Education, School of Chemistry, Beihang University, Beijing 100191, P. R. China. E-mail: liuzy@buaa.edu.cn*

[b]*Key Laboratory of Micro-Nano Measurement-Manipulation and Physics (Ministry of Education), School of Physics, Beihang University, Beijing 100191, P. R. China. E-mail: liwp@buaa.edu.cn*

[c]*Guangdong Provincial Key Laboratory of Optical Information Materials and Technology, South China Academy of Advanced Optoelectronics, South China Normal University, Guangzhou 510006, P. R. China. E-mail: wangyao@m.scnu.edu.cn*

† Electronic supplementary information (ESI) available: SEM images, current–voltage curves, theoretical model. See DOI: 10.1039/d0ra01145b

‡ Rifeng Luo and Tianliang Xiao contributed equally to this work.

quality layered GO membrane by a simple vacuum filtration (Fig. 1A).[48,49] In our work, GO nanosheets with a lateral size of several hundred of nanometers and a thickness of ~1.1 nm (Fig. 1B and C) were vacuum-filtrated into a paper-like layered membrane with a thickness of ~6.5 μm. The self-standing GO membrane showed the typical features of a wrinkled surface and a layered cross section (Fig. 1D and E). The side of GO membrane that was exposed to air during vacuum filtration was defined as a front side, while the other side that was in contact with the filter was defined as a back side. After the front side of GO membrane was exposed to pyrrole vapor for a spontaneous polymerization for 8 h, the membrane color changed from brown to black because of the deposition of polypyrrole (Fig. 1A). It has been recognized that the oxygen-containing groups on the surface of GO nanosheets were able to oxidize the pyrrole monomers into polypyrrole, which were deposited into the interlayer spaces of GO membrane.[55] The deposition of polypyrrole made the surface of the front side of GO membrane become slightly smooth, while the morphology of the cross-section remained almost unchanged (ESI, Fig. S1†).

The formation of polypyrrole on GO membrane was characterized by Fourier transform infrared spectroscopy (FTIR). Fig. 2A depicted the appearance of characteristic vibration peaks of polypyrrole in modified GO membrane. The C–N stretching vibration was observed at 1216 cm^{-1} and the out of plane deformation vibration of C–H was shown at 931 cm^{-1}.[56] The weak signals of FTIR characteristic peaks was ascribed to the small amount of polypyrrole in GO membrane. On the basis of X-ray diffraction pattern (Fig. 2B), we calculated the interlayer spacing (d_{002}) of the GO membrane was 0.77 nm ($2\theta = 11.4°$) according to Bragg's equation ($n\lambda = 2d \sin\theta$), which acted as fluidic channels for the ion transport. This small interlayer

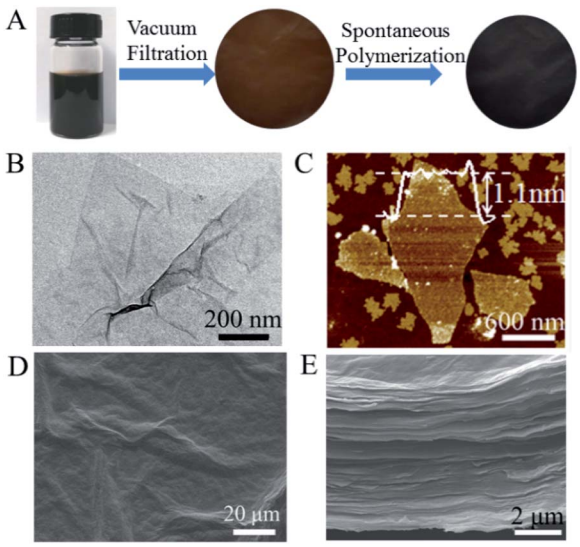

Fig. 1 (A) Photographs of graphene oxide (GO) dispersion solution, vacuum-filtered GO membrane and polypyrrole-modified GO membrane (GO/PPy). (B and C) TEM (B) and AFM (C) images of GO nanosheets. (D and E) Top-viewed (D) and cross-sectional (E) SEM images of GO membrane.

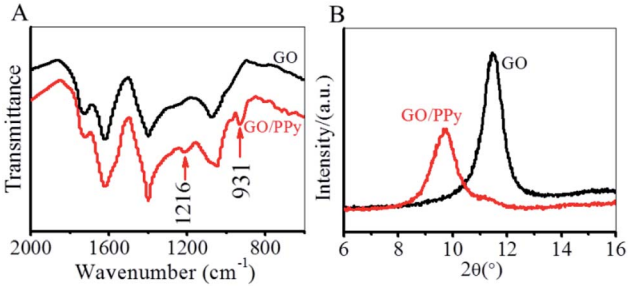

Fig. 2 (A) FTIR spectra of GO and GO/PPy membrane. The characteristic vibration peaks of polypyrrole in GO/PPy membrane were identified. (B) XRD pattern of GO and GO/PPy membrane. The interlayer spacing increased after polypyrrole modification.

spacing of GO membrane provided a small space for polypyrrole intercalation, which resulted in a small amount of polypyrrole deposited in GO membrane. After polypyrrole modification, the interlayer spacing of polypyrrole-modified GO membrane increased to be 0.91 nm calculated from the diffraction peak at $2\theta = 9.7°$. This increased interlayer spacing implied the intercalation of polypyrrole into the GO membrane.

The asymmetric modification of polypyrrole on the two sides of GO membrane was characterized by the measurements of water contact angles (CAs) and Raman spectra. As shown in Fig. 3A, the water CAs on the front and back sides of GO membrane were 67° and 77° respectively. This slight difference in the CAs was ascribed to the different morphology of the two sides (Fig. S2†). After GO membrane was modified with polypyrrole, the water CA of the front side of GO membrane increased to be 86°, while that of the back side remained almost unchanged (79°). This difference in water CAs on the two sides identified the asymmetric modification of polypyrrole. Such an asymmetry was further identified by Raman spectra. As shown in Fig. 3B, the characteristic peaks of graphene appeared at 1346 cm^{-1} (D-band) and 1593 cm^{-1} (G-band). After polypyrrole modification, several new peaks with low intensity between 800 cm^{-1} and 1200 cm^{-1} were detected on the front side of GO membrane, which was assigned to polypyrrole.[57] On the contrary, almost no peaks were detected for polypyrrole on the

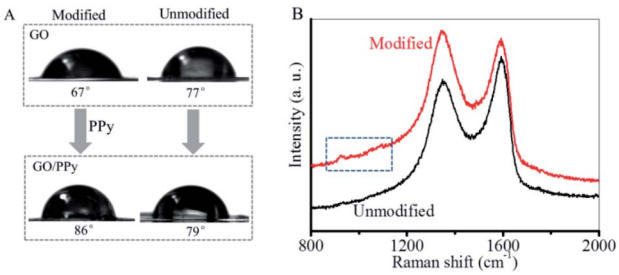

Fig. 3 Characterization of the asymmetric modification of polypyrrole on the two sides of polypyrrole-modified GO membrane (GO/PPy). (A) The water contact angles (CAs) on the two sides of GO and GO/PPy membrane. The polypyrrole modification increased the water CA. (B) Raman spectra of the two sides of GO/PPy membrane. The new peaks between 800 cm^{-1} and 1200 cm^{-1} were assigned to polypyrrole.

back side. Our results indicated that polypyrrole was mainly formed on the front side of GO membrane, which resulted in an asymmetry in polypyrrole distribution.

The polypyrrole-modified GO membrane was then mounted between two electrochemical cells containing 1 mM of KCl aqueous solution with a pH value of 6.8 to form an ionic diode. The ion rectification behavior was investigated by measuring the current–voltage (I–V) curves.[58,59] As shown in Fig. 4A, when a transmembrane voltage of −2 to +2 V was applied across the membrane, a nonlinear I–V curve indicating an ion rectification behavior was obtained. The ion rectification ratio (f_R) was defined as the ratio between the absolute values of ion current at +2 V(I_{+2}) and at −2 V(I_{-2}), that is $f_R = |I_{+2}|/|I_{-2}|$. At +2 V voltage, an ion current of 0.17 μA was obtained, which was much higher than that at −2 V (−0.08 μA). The rectification ratio was calculated to be ~2.1. The ion ionic diode remained at an "open" state at a positive voltage, while remained at a "closed" state at a negative voltage, showing a diode behavior. The ion rectification behavior could be ascribed to the asymmetric modification of polypyrrole (PPy) on GO membrane (Fig. 4B). In 1 mM of KCl aqueous solution (pH ~6.8), the nanoscaled interlayer spacing (~0.91 nm) of GO membrane was much smaller than the Debye length (~9.6 nm) of the electrolyte. Therefore, the negatively charged surface of GO nanosheets by carboxylic groups ($pK_a \sim 3.8$) makes GO membrane show cationic selectivity. After the neutral polypyrrole was mainly deposited on the front side of GO membrane, the occupation of interlayer space by polypyrrole was reasonably considered to result in an asymmetry in the channel size for ion transport (Fig. 4B). While the surface charges of GO remained unchanged.

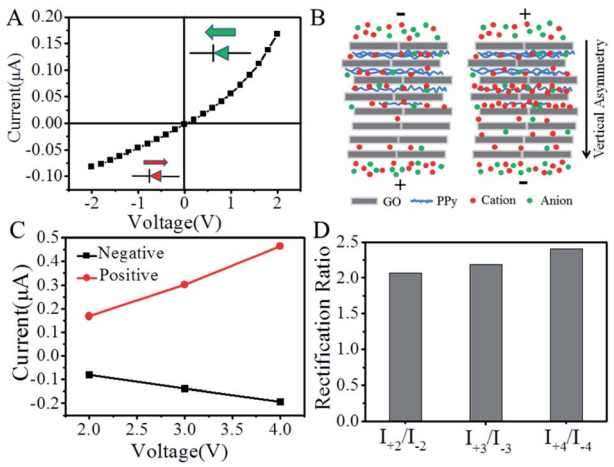

Fig. 4 (A) Ion current–voltage (I–V) curve of an ionic diode based on polypyrrole-modified GO membrane in 1 mM of KCl aqueous solution. The ionic diode remains at an "open" state at a positive voltage, while remains at a "closed" state at a negative voltage, showing a diode behavior. (B) The formation of ion depletion in the unmodified GO side at a negative voltage and ion enrichment in the modified GO side at a positive voltage. The asymmetric distribution of polypyrrole in the GO membrane resulted in an asymmetry in the channel size for ion transport. The diagram was not drawn to scale. (C) The dependence of ion current on the applied positive and negative voltages. (D) The ion rectification ratio of the ionic diode under different voltage range.

When a negative transmembrane voltage was applied across the polypyrrole-modified membrane, ion depletion was formed in the unmodified GO side because of the high cationic concentration in the modified GO side (Fig. 4B). In this case, the ion ionic diodes remained at a "closed" state with a low ion current. On the contrary, a positive transmembrane voltage resulted in ion enrichment in the modified GO side, which made the ionic diodes remain at an "open" state showing a high ion current (Fig. 4B). Overall, the voltage-induced ion enrichment and ion depletion rectified the ion transport through the polypyrrole-modified GO membrane.

The ionic diode that shows an ion rectification property over a wide voltage range is essentially important for their applications at high applied voltage. Therefore, we investigated the ion rectification behavior of the ionic diode under different range of transmembrane voltage (ESI, Fig. S3†). As shown in Fig. 4C, following the increase of applied positive voltage from +2 to +4 V, the ion current increased linearly from 0.17 μA to 0.47 μA. Correspondingly, the increase in the applied negative voltage from −2 V to −4 V made the ion current increase linearly from 0.08 μA to 0.19 μA. As a result, the ion rectification ratio was 2.1, 2.2 and 2.4 respectively at a voltagerange of −2 to +2 V, −3 to +3 V and −4 to +4 V (Fig. 4D). These results indicated that our ionic diode could remain a stable ion rectification property over a wide voltage range.

The role of polypyrrole asymmetry in the ion rectification property of polypyrrole-modified GO membrane was theoretically investigated by a calculation based on Poisson–Nernst–Planck equations.[30,31] The modified GO membrane was theoretically modeled as a cylindrical single nanochannel with a total length of 2000 nm. Fig. 5A showed the axial section of the cylindrical nanochannels. The colored part represented the hollow interior of the nanochannels, while the white wide line represented the neutral polypyrrole in the nanochannels. The

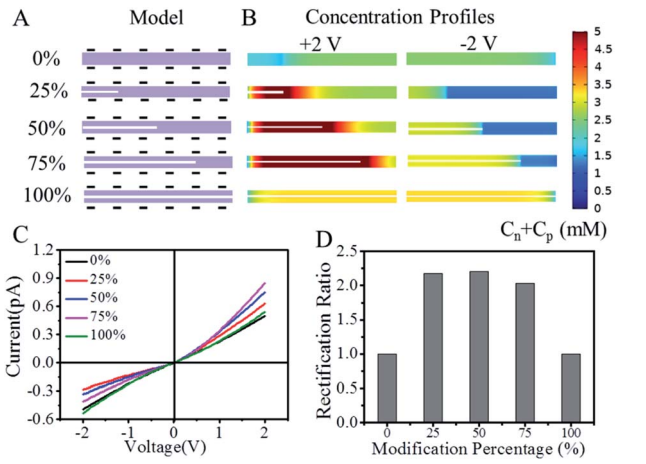

Fig. 5 Theoretical simulations of the ion transport properties of polypyrrole-modified GO membrane with different modification percentage. (A) The simplified model with polypyrrole modification percentage of 0%, 25%, 50%, 75% and 100%. (B) The calculated ion concentration profiles at +2 V and −2 V voltages. (C) The simulated I–V curves. (D) The corresponding rectification ratios.

increase in the length of wide line implied the increase in the modification percentage of neutral polypyrrole. The pore sizes of unmodified and modified nanochannel in the model were set to be 28 nm and 12 nm respectively. Then, the role of polypyrrole with modified percentage of 25%, 50%, 75% and 100% of the total length was investigated by calculating the ion current–voltage curves and ion concentration profiles (Fig. 5A). Comparing with unmodified nanochannels, the asymmetric modification of polypyrrole induced ion enrichment at a positive voltage and ion depletion at a negative voltage (Fig. 5B), resulting in nonlinear *I–V* curves (Fig. 5C). When the polypyrrole percentage was 25%, an ion rectification ratio of 2.18 was obtained (Fig. 5D). The increase of polypyrrole percentage to 50% slightly increased the ion rectification ratio to be 2.21. Following the further increase of polypyrrole percentage to 75%, the ion rectification decreased slightly to be 2.03 due to the weakened geometric asymmetry. When the nanochannel was completely modified by polypyrrole (*i.e.* the modified percentage was 100%), the ion enrichment at a positive voltage and ion depletion at a negative voltage disappeared, resulting in a linear *I–V* curve. Our calculated results implied that the polypyrrole asymmetry was essentially important for the ion rectification property. However, the modified percentage of polypyrrole showed a small effect on the ion rectification ratio possibly because of the weak asymmetry and the low charge density.

3. Experimental

3.1 Fabrication of polypyrrole-modified GO membrane

A GO dispersion aqueous solution with a concentration of 2 mg mL^{-1} was commercially available from Nanjing MKNANO Co., Ltd. (China). A layered GO membrane was obtained by a vacuum filtration of GO dispersion solution through a mixed cellulose ester filter membrane (25 mm diameter and 450 nm pore size, Shanghai Xinya Company, China). Subsequently, a self-standing GO membrane was obtained by peeling off it from the filter. The side of GO membrane that was exposed to air during vacuum filtration was defined as a front side, while the other side that was in contact with the filter was defined as a back side. For the modification of polypyrrole, the front side of GO membrane was exposed to the environment filled with pyrrole vapor (J&K Scientific Ltd., China), while the back side was adhered to a glass substrate with an adhesive tape to avoid being exposed to the pyrrole vapor.[55] After a spontaneous oxidation polymerization for 8 h, polypyrrole was mainly modified on the front side of GO membrane.

3.2 Characterization

The morphology of GO nanosheets was observed with a FEI JEM-1200EX transmission electron microscope (TEM). The thickness of GO nanosheets was determined with a Bruker Dimension Icon atomic force microscope (AFM). A FEI Quanta FEG 250 environmental scanning electron microscope (SEM) was used to observe the surface and cross-sectional morphology of the GO membrane. The interlayer spacing of GO membranes was calculated based on the X-ray diffraction pattern (XRD) measured by an Ultima IV X-ray diffraction meter (Rigaku Corporation, Japan). A Nicolet IS10 transform infrared spectroscopy (FTIR) spectrometer was used to characterize the compositions of polypyrrole. Water contact angle (CA) measurements were performed using a POWEREACH JC2000D1 contact-angle system (Shanghai Zhongchen Co., Ltd., China). Raman spectra were measured by a Renishaw inVia spectrometer with a 532 nm laser excitation.

3.3 Electric measurements

The polypyrrole-modified GO membrane was mounted between two electrochemical cells to form an ionic diode.[58,59] The ion rectification of ionic diode was investigated by measuring the current–voltage (*I–V*) curves in 1 mM of KCl aqueous solution with a pH value of 6.8 using a Keithley 6487 picoammeter (Keithley Instruments, Cleveland, OH). A couple of Ag/AgCl electrodes were used to apply a transmembrane voltage across the membrane. The anode was fixed to face the polypyrrole-modified side and the cathode faced to the other side.

3.4 Model simulation

The ion rectification of ionic diodes was simulated by using "Electrostatics" and "Transport of Diluted Species" modules in COMSOL Multiphysics 5.4.[30,31] The polypyrrole-modified GO membrane was theoretically modeled as a cylindrical single nanochannel with an asymmetric structure, which was shown in Fig. S4 (ESI†). The total length of nanochannel was set to be 2000 nm. The modified percentage of polypyrrole was supposed to be 25%, 50%, 75% and 100% of the total length. The pore sizes of unmodified and modified nanochannel were set to be 28 nm and 12 nm respectively. After setting the density of surface negative charges on GO to be -0.001 C m^{-2}, the ion current–voltage curves and ion concentration profiles were obtained.

4. Conclusions

In summary, an ionic diode based on a polypyrrole-modified GO membrane was described. The asymmetric geometry in a vertical dimension was achieved by the spontaneous oxidation polymerization of pyrrole monomers on one side of GO membrane in vapor phase, which resulted in an asymmetric geometry due to the occupation of interlayer space of one side of GO membrane by polypyrrole. The resulted ionic diode demonstrated an obvious ionic rectification behavior over a wide voltage range. A theoretical calculation based on the Poisson–Nernst–Planck equations implied that the asymmetric modification of polypyrrole was essentially important for the ion rectification property.

Conflicts of interest

There are no conflicts to declare.

Acknowledgements

This work was supported by National Natural Science Foundation of China (21571011, 21975011), National Key Research and Development Program of China (2017YFA0206902, 2017YFA0206900), the Guangdong Provincial Key Laboratory of Optical Information Materials and Technology (2017B030301007) and the Fundamental Research Funds for the Central Universities (YWF-20-BJ-J-416). We thank Dr Daibing Luo from Analytical & Testing Center of Sichuan University for technical support.

Notes and references

1 Z. S. Siwy and S. Howorka, *Chem. Soc. Rev.*, 2010, **39**, 1115–1132.
2 X. Hou, W. Guo and L. Jiang, *Chem. Soc. Rev.*, 2011, **40**, 2385–2401.
3 Z. Zhang, L. Wen and L. Jiang, *Chem. Soc. Rev.*, 2018, **47**, 322–356.
4 X. Hou, *Adv. Mater.*, 2016, **28**, 7049–7064.
5 G. Pérez-Mitta, M. E. Toimil-Molares, C. Trautmann, W. A. Marmisollé and O. Azzaroni, *Adv. Mater.*, 2019, **31**, 1901483.
6 L. Lin, J. Yan and J. Li, *Anal. Chem.*, 2014, **86**, 10546–10551.
7 L. Lin, L. Zhang, L. Wang and J. Li, *Chem. Sci.*, 2016, **7**, 3645–3648.
8 Z. Zhu, D. Wang, Y. Tian and L. Jiang, *J. Am. Chem. Soc.*, 2019, **141**, 8658–8669.
9 K. Xiao, L. Jiang and M. Antonietti, *Joule*, 2019, **3**, 2364–2380.
10 M. Ali, I. Ahmed, S. Nasir, P. Ramirez, C. M. Niemeyer, S. Mafe and W. Ensinger, *ACS Appl. Mater. Interfaces*, 2015, **7**, 19541–19545.
11 G. Laucirica, W. A. Marmisolle, M. E. Toimil-Molares, C. Trautmann and O. Azzaroni, *ACS Appl. Mater. Interfaces*, 2019, **11**, 30001–30009.
12 W. Hsu and H. Daiguji, *Anal. Chem.*, 2016, **88**, 9251–9258.
13 I. Boussouar, Q. Chen, X. Chen, Y. Zhang, F. Zhang, D. Tian, H. S. White and H. Li, *Anal. Chem.*, 2017, **89**, 1110–1116.
14 C. Lin, C. Combs, Y. Su, L. Yeh and Z. S. Siwy, *J. Am. Chem. Soc.*, 2019, **141**, 3691–3698.
15 C. Lin, T. Ma, Z. Siwy, S. Balme and J. Hsu, *J. Phys. Chem. Lett.*, 2020, **11**, 60–66.
16 L. Tshwenya, F. Marken, K. Mathwig and O. Arotiba, *ACS Appl. Mater. Interfaces*, 2020, **12**, 3214–3224.
17 W. Huang and J. Hsu, *J. Colloid Interface Sci.*, 2019, **557**, 683–690.
18 B. R. Putra, K. J. Aoki, J. Chen and F. Marken, *Langmuir*, 2019, **35**, 2055–2065.
19 G. Laucirica, V. M. Cayón, Y. T. Terrones, K. L. Cortez, M. E. Toimil-Molares, C. Trautmann, W. A. Marmisollé and O. Azzaroni, *Nanoscale*, 2020, **12**, 6002–6011.
20 M. Ali, P. Ramirez, S. Nasir, J. Cervera, S. Mafe and W. Ensinger, *Soft Matter*, 2019, **15**, 9682–9689.
21 C. Wei, A. J. Bard and S. W. Feldberg, *Anal. Chem.*, 1997, **69**, 4627–4633.
22 Z. Siwy, P. Apel, D. Baur, D. D. Dobrev, Y. E. Korchev, R. Neumann, R. Spohr, C. Trautmann and K. Voss, *Surf. Sci.*, 2003, **532–535**, 1061–1066.
23 Z. Siwy, I. D. Kosińska, A. Fuliński and C. R. Martin, *Phys. Rev. Lett.*, 2005, **94**, 048102.
24 Z. Siwy, E. Heins, C. C. Harrell, P. Kohli and C. R. Martin, *J. Am. Chem. Soc.*, 2004, **126**, 10850–10851.
25 Z. Siwy, Y. Gu, H. A. Spohr, D. Baur, A. Wolf-Reber, R. Spohr, P. Apel and Y. E. Korchev, *Europhys. Lett.*, 2002, **60**, 349–355.
26 W. Lan, D. A. Holden and H. S. White, *J. Am. Chem. Soc.*, 2011, **133**, 13300–13303.
27 Z. Jiang, H. Liu, S. A. Ahmed, S. Hanif, S. Ren, J. Xu, H. Chen, X. Xia and K. Wang, *Angew. Chem., Int. Ed.*, 2017, **56**, 4767–4771.
28 R. Fang, H. Zhang, L. Yang, H. Wang, Y. Tian, X. Zhang and L. Jiang, *J. Am. Chem. Soc.*, 2016, **138**, 16372–16379.
29 K. Xiao, G. Xie, Z. Zhang, X. Kong, Q. Liu, P. Li, L. Wen and L. Jiang, *Adv. Mater.*, 2016, **28**, 3345–3350.
30 I. Vlassiouk, S. Smirnov and Z. Siwy, *ACS Nano*, 2008, **2**, 1589–1602.
31 H. Daiguji, Y. Oka and K. Shirono, *Nano Lett.*, 2005, **5**, 2274–2280.
32 R. Karnik, C. Duan, K. Castelino, H. Daiguji and A. Majumdar, *Nano Lett.*, 2007, **7**, 547–551.
33 R. Yan, W. Liang, R. Fan and P. Yang, *Nano Lett.*, 2009, **9**, 3820–3825.
34 C. Li, F. Ma, Z. Wu, H. Gao, W. Shao, K. Wang and X. Xia, *Adv. Funct. Mater.*, 2013, **23**, 3836–3844.
35 S. Wu, F. Wildhaber, O. Vazquez-Mena, A. Bertsch, J. Brugger and P. Renaud, *Nanoscale*, 2012, **4**, 5718–5723.
36 Y. Jiang, Y. Feng, J. Su, J. Nie, L. Cao, L. Mao, L. Jiang and W. Guo, *J. Am. Chem. Soc.*, 2017, **139**, 18739–18746.
37 I. Vlassiouk and Z. S. Siwy, *Nano Lett.*, 2007, **7**, 552–556.
38 I. Vlassiouk, T. R. Kozel and Z. S. Siwy, *J. Am. Chem. Soc.*, 2009, **131**, 8211–8220.
39 J. Gao, W. Guo, D. Feng, H. Wang, D. Zhao and L. Jiang, *J. Am. Chem. Soc.*, 2014, **136**, 12265–12272.
40 K. Xiao, L. Chen, Z. Zhang, G. Xie, P. Li, X. Kong, L. Wen and L. Jiang, *Angew. Chem., Int. Ed.*, 2017, **56**, 8168–8172.
41 M. Miansari, J. R. Friend, P. Banerjee, M. Majumder and L. Y. Yeo, *J. Phys. Chem. C*, 2014, **118**, 21856–21865.
42 M. Miansari, J. R. Friend and L. Y. Yeo, *Adv. Sci.*, 2015, **2**, 1500062.
43 S. T. Martin, A. Neild and M. Majumder, *APL Mater.*, 2014, **2**, 092803.
44 L. Wang, Y. Feng, Y. Zhou, M. Jia, G. Wang, W. Guo and L. Jiang, *Chem. Sci.*, 2017, **8**, 4381–4386.
45 W. Fei, M. Xue, H. Qiu and W. Guo, *Nanoscale*, 2019, **11**, 1313–1318.
46 X. Zhang, Q. Wen, L. Wang, L. Ding, J. Yang, D. Ji, Y. Zhang, L. Jiang and W. Guo, *ACS Nano*, 2019, **13**, 4238–4245.
47 J. Gao, Y. Feng, W. Guo and L. Jiang, *Chem. Soc. Rev.*, 2017, **46**, 5400–5424.
48 J. Ji, Q. Kang, Y. Zhou, Y. Feng, X. Chen, J. Yuan, W. Guo, Y. Wei and L. Jiang, *Adv. Funct. Mater.*, 2017, **27**, 1603623.
49 K. Raidongia and J. Huang, *J. Am. Chem. Soc.*, 2012, **134**, 16528–16531.

50 Q. Zhang, Z. Liu, K. Wang and J. Zhai, *Adv. Funct. Mater.*, 2015, **25**, 2091–2098.
51 Q. Zhang, Z. Zhang, H. Zhou, Z. Xie, L. Wen, Z. Liu, J. Zhai and X. Diao, *Nano Res.*, 2017, **10**, 3715–3725.
52 G. Pérez-Mitta, W. A. Marmisollé, C. Trautmann, M. E. Toimil-Molares and O. Azzaroni, *Adv. Mater.*, 2017, **29**, 1700972.
53 B. Bao, J. Hao, X. Bian, X. Zhu, K. Xiao, J. Liao, J. Zhou, Y. Zhou and L. Jiang, *Adv. Mater.*, 2017, **29**, 1702926.
54 G. Pérez-Mitta, W. A. Marmisollé, C. Trautmann, M. E. Toimil-Molares and O. Azzaroni, *J. Am. Chem. Soc.*, 2015, **137**, 15382–15385.
55 Y. Jiang, C. Hu, H. Cheng, C. Li, T. Xu, Y. Zhao, H. Shao and L. Qu, *ACS Nano*, 2016, **10**, 4735–4741.
56 X. Nie, T. Xiao and Z. Liu, *Chem. Commun.*, 2019, **55**, 10023–10026.
57 Y. Zhao, J. Liu, Y. Hu, H. Cheng, C. Hu, C. Jiang, L. Jiang, A. Cao and L. Qu, *Adv. Mater.*, 2013, **25**, 591–595.
58 N. Yan, T. Xiao and Z. Liu, *Acta Chim. Sin.*, 2017, **75**, 873–877.
59 T. Xiao, J. Ma, J. Jiang, M. Gan, B. Lu, R. Luo, Q. Liu, Q. Zhang, Z. Liu and J. Zhai, *Chem.–Eur. J.*, 2019, **25**, 12795–12800.

